

Provided for non-commercial research and education use.  
Not for reproduction, distribution or commercial use.



**This article was published in an Elsevier journal. The attached copy is furnished to the author for non-commercial research and education use, including for instruction at the author's institution, sharing with colleagues and providing to institution administration.**

**Other uses, including reproduction and distribution, or selling or licensing copies, or posting to personal, institutional or third party websites are prohibited.**

**In most cases authors are permitted to post their version of the article (e.g. in Word or Tex form) to their personal website or institutional repository. Authors requiring further information regarding Elsevier's archiving and manuscript policies are encouraged to visit:**

**<http://www.elsevier.com/copyright>**



# Understanding cyclical thrombocytopenia: A mathematical modeling approach

Raluca Apostu<sup>a,\*</sup>, Michael C. Mackey<sup>b</sup>

<sup>a</sup>*Department of Mathematics and Statistics & Centre for Nonlinear Dynamics in Physiology and Medicine, McGill University,  
3655 Promenade Sir William Osler, Montreal, QC, Canada H3G 1Y6*

<sup>b</sup>*Departments of Physiology, Physics & Mathematics and Centre for Nonlinear Dynamics in Physiology and Medicine, McGill University,  
3655 Promenade Sir William Osler, Montreal, QC, Canada, H3G 1Y6*

Received 14 August 2007; received in revised form 16 November 2007; accepted 26 November 2007

Available online 11 January 2008

---

## Abstract

Cyclical thrombocytopenia (CT) is a rare hematological disease characterized by periodic oscillations in the platelet count. Although first reported in 1936, the pathogenesis and an effective therapy remain to be identified. Since besides fluctuations in platelet levels the patients hematological profile have been consistently normal, a destabilization of a peripheral control mechanism might play an important role in the genesis of this disorder. In this paper, we investigate through computer simulations the mechanisms underlying the platelet oscillations observed in CT. First, we collected the data published in the last 40 years and quantified the significance of the platelet fluctuations using Lomb–Scargle periodograms. Our analysis reveals that the incidence of the statistically significant periodic data is equally distributed in men and women. The mathematical model proposed in this paper captures the essential features of hematopoiesis and successfully duplicates the characteristics of CT. With the same parameter changes, the model is able to fit the platelet counts and to qualitatively reproduce the TPO oscillations (when data is available). Our results indicate that a variation in the megakaryocyte maturity, a slower relative growth rate of megakaryocytes, as well as an increased random destruction of platelets are the critical elements generating the platelet oscillations in CT.

© 2007 Elsevier Ltd. All rights reserved.

*Keywords:* Cyclical thrombocytopenia; Platelet oscillations; Delay differential equations; Spectral data analysis; Mathematical model

---

## 1. Introduction

All blood cells arise from a common origin in the bone marrow, the hematopoietic stem cells (HSC). HSC are morphologically undifferentiated cells which can either proliferate or differentiate to produce all types of blood cells (erythrocytes, neutrophils and platelets). The proliferation of the stem cells and progenitor cells is controlled by a negative feedback system mediated by hematopoietic cytokines. Erythropoietin (EPO) is the hormone that mediates the RBC production, granulocyte colony stimulating factor (G-CSF) controls the regulation of neutrophils, and thrombopoietin (TPO) known as C-Mpl ligand

or megakaryocyte growth and development factor, is the primary regulator of thrombopoiesis.

Hematopoiesis is a homeostatic system and, consequently, most disorders of its regulation lead to chronic failures in the production of either all or only one blood cell type. Among the wide range of diseases affecting the blood cells, there are some which are characterized by predictable oscillations in one or more cellular elements of the blood. They are called periodic or dynamical diseases (Glass and Mackey, 1988). The investigation of their dynamic character offers an opportunity to enrich our knowledge about some regulation processes of blood cell production and may suggest better therapeutic strategies (Foley et al., 2006). Cyclical neutropenia (Colijn and Mackey, 2005a; Haurie et al., 1998, 1999, 2000), periodic chronic myelogenous leukemia (Colijn and Mackey, 2005a; Fortin and Mackey, 1999), periodic autoimmune

---

\*Corresponding author. Tel.: +1 514 398 8092; fax: +1 514 398 7452.  
E-mail address: [raluca.apostu@mail.mcgill.ca](mailto:raluca.apostu@mail.mcgill.ca) (R. Apostu).

hemolytic anemia (Mackey and Glass, 1977) and cyclical thrombocytopenia (CT) (Swinburne and Mackey, 2000) are some classical examples of dynamical hematological diseases. Diseases like periodic chronic myelogenous leukemia (PCML) and cyclical neutropenia (CN), which involve fluctuations in all major blood cell lines with the same period on a given subject, are believed to arise in the stem cell compartment in the bone marrow. Since in CT or periodic autoimmune hemolytic anemia besides oscillations in one type of cell count the patients hematological profile have been consistently normal, a destabilization of a peripheral control mechanism might play an important role in the genesis of this disorders.

Of particular interest in this paper is CT. CT is a rare hematological disorder described mostly in adults and characterized by periodic platelet count fluctuations of unknown etiology. It seems to occur predominantly in women but the incidence of the statistically significant periodic platelet data is equally distributed between men and women. Sometimes this disease is associated with bleeding symptoms which have no apparent cause other than thrombocytopenia (low platelet count): purpura, petechiae, epistaxis, gingival bleeding, menorrhagia, easy bruising and gastrointestinal bleeding. Although, in general, human platelet levels remain relatively stable for years ( $150 \times 10^9$ – $450 \times 10^9$  platelets/L with an average of  $290 \times 10^9$  platelets/L), many factors can influence an individual's platelet count (e.g. exercise, racial origin, some diseases, pregnancy). In CT the platelet counts oscillate from very low ( $1 \times 10^9$  platelets/L) to normal or very high levels ( $2000 \times 10^9$  platelets/L). This hematological disorder was reviewed by Go (2005), Swinburne and Mackey (2000), Cohen and Cooney (1974), and has been the subject of mathematical modeling (Santillán et al., 2000; Von Schulthess and Gessner, 1986). Our goal is to investigate through computer simulations CT and to formulate a hypothesis of the mechanisms underlying the platelet fluctuations. For this purpose we develop a mathematical model which captures the essential characteristics of hematopoiesis and offers an advantage comparable with the earlier models consisting of one cell line or one line coupled to the stem cells.

This paper is organized as follows. Section 1 presents a brief overview of CT. In Section 2 we quantify the platelet oscillations using Lomb–Scargle periodograms. The mathematical model developed in Section 4 is used to explore the origin of the rhythmic fluctuations which characterize CT. A detailed numerical analysis of the model dynamics allows us to zoom in the parameter space, and to identify the parameters with essential role in generating a model response similar with CT data (Section 4.1). Section 4.2 reveals that the hematopoietic model successfully duplicates the platelet counts of CT patients, and provides a qualitative fitting of the TPO levels when they were available. The biological interpretation of the results, the comparison with the clinical findings, and the conclusions

drawn from the previous modeling effort are presented in the last two sections.

### 1.1. Cyclical thrombocytopenia

Since the first report of Minot (1936), many CT patients have been described. Searching the English literature from 1962 to 2005 we found 38 well-documented cases of platelet fluctuations (34 putative patients and four healthy individuals). All the reports have been sporadic, except for an apparently unique family described by Aranda and Dorantes (1977), in which the platelet cycling was observed in four out of nine siblings and their father. Some of these studies presented patients without any treatment (Aranda and Dorantes, 1977; Lewis, 1974; Rice et al., 2001; Wilkinson and Firkin, 1966; Zent et al., 1999), and others described subjects undergoing various therapies.

The pathogenesis of CT is poorly understood and various mechanism have been proposed. The clinical findings suggest at least two pathways: immune-mediated platelet destruction (autoimmune CT) and megakaryocyte deficiency and cyclical failure in platelet production (amegakaryocytic CT). Autoimmune CT is thought to be an unusual form of immune thrombocytopenia purpura (ITP) and is more common in females. The hematological profile of most of these patients reveals high levels of antiplatelet antibodies, shorter platelet lifespan at the platelet nadir and normal to high levels of marrow megakaryocytes. Amegakaryocytic CT is postulated to be a variant of acquired amegakaryocytic thrombocytopenic purpura and is mainly characterized by the absence of megakaryocytes in the thrombocytopenia phase and increased megakaryocyte number during thrombocytosis. Serial tests for serum antiplatelet antibodies are negative and the platelet lifespan is normal. To determine the cause of cyclic megakaryocytopenia, Nagasawa et al. (1998) examined the integrity of the megakaryocyte progenitor compartment just prior to the nadir and the peak of platelet cycle. They noticed that in the autoimmune case the mean size of megakaryocytes does not change with the cyclic variations in the platelet count, while in patients with the amegakaryocytic variety the number of colony-forming unit-megakaryocyte (CFU-Meg), the megakaryocyte number, and the cytoplasmic area fluctuated with the platelet cycle. In all reported cases, except for Füreder et al. (2002) and Menitove et al. (1989), besides oscillations in platelet count, the patient's hematological profile has been consistently normal. The peripheral red and white blood cell counts were within the normal range, and the blood smear shows no morphological abnormalities or platelet clumps. In the case presented by Füreder et al. (2002), erythropoiesis and granulopoiesis were slightly affected. The Menitove et al. (1989) patient manifested a severe iron deficiency with anemia and reticulocytosis. A synchronization between the fluctuations in the platelet count and menses has been reported in some female patients (Helleberg, 1995; Minot, 1936; Tomer et al., 1989). The fact that CT occurs

also in men and females after menopause indicates that the pathogenesis of this disorder is not necessarily related to the menstrual cycle. For example, Cohen and Cooney (1974) observe that platelet cycles are in phase with their patient's menstrual cycle only when she was under exogenous hormone therapy, while other groups of investigators (Hoffman et al., 1989; Menitove et al., 1989; Yanabu et al., 1993) report no correlation between platelet oscillations and menses.

## 2. Spectral analysis of platelet data

We tested all data sets for the presence of statistically significant periodicity in the platelet counts. Since the time series are unevenly sampled and may contain random measurement errors, the best way of extracting information about the oscillatory components is through Lomb–Scargle periodogram (Lomb, 1976; Scargle, 1982; Press et al., 1993). Specifically, let  $x_j$  be the concentration of the platelets as measured at time  $t_j$ ,  $j = \overline{1, N}$ , where  $N$  is the number of total data points. As usual, the mean and variance of data values are defined by

$$\bar{x} = \frac{1}{N} \sum_{j=1}^N x_j \quad \text{and} \quad \sigma^2 = \frac{1}{N-1} \sum_{j=1}^N (x_j - \bar{x})^2.$$

The Lomb–Scargle periodogram (also called Lomb normalized periodogram) defines the spectral power  $P(\omega)$  as a function of the angular frequency  $\omega = 2\pi f$  by the following formula:

$$P(\omega) = \frac{1}{2\sigma^2} \left\{ \frac{(\sum_{j=1}^N (x_j - \bar{x}) \cos \omega(t_j - \rho))^2}{\sum_{j=1}^N \cos^2 \omega(t_j - \rho)} + \frac{(\sum_{j=1}^N (x_j - \bar{x}) \sin \omega(t_j - \rho))^2}{\sum_{j=1}^N \sin^2 \omega(t_j - \rho)} \right\}, \quad (1)$$

where  $\rho$  is a constant defined implicitly by

$$\tan(2\omega\rho) = \frac{\sum_{j=1}^N \sin(2\omega t_j)}{\sum_{j=1}^N \cos(2\omega t_j)}.$$

The value of  $P(\omega)$  indicates the likelihood of a periodicity with period  $P = \frac{2\pi}{\omega} = \frac{1}{f}$  in the data set. To determine the presence or absence of a periodic signal we need to quantify the significance of a peak in the periodogram. Given the null hypothesis that the values  $x_j$  are independent Gaussian random values, and that  $P(\omega)$  has an exponential probability distribution with unit mean, the significance level  $p$  of every peak in a periodogram is given by

$$p = 1 - (1 - e^{-P(\omega)})^M, \quad (2)$$

where  $M$  represents the number of independent frequencies. In our work, an individual data set is considered periodic if the significance level  $p$  of the principal peak in the periodogram is less than 0.05.

The spectral analysis of the platelet counts is displayed graphically in Appendix A, where each data set is identified

as to source. Based on our criterion for statistical significance, only 22 out of 38 data sets are significantly periodic (11 males and 11 females). The period of platelet oscillations varies between individuals, with a shorter average period in women ( $26 \pm 10$  days) compared to men ( $35 \pm 12$  days). There is a connection between the patient's diagnosis and the range of significant periods of platelet variations. The oscillations in autoimmune data have periods ranging from 13 to 31 days which, on average, are shorter than the periods in amegakaryocytic cases. The latter vary from 19 to 64 days. Table 1 summarizes the results of our data analysis. For each patient we specify the sex, the diagnosis, and the significant period(s).

## 3. A mathematical model of hematopoiesis

Recently, Colijn and Mackey (2005b) synthesized a  $G_0$ -type model for the HSC dynamics (Mackey, 1978) with the mathematical models for leukocyte (Bernard et al., 2003; Haurie et al., 2000; Hearn et al., 1998), erythrocyte (Bélair et al., 1995; Mackey, 1979; Mahaffy et al., 1998), and platelet production (Bélair and Mackey, 1987; Santillán et al., 2000) into a comprehensive model of hematopoiesis. Since their model has been shown to display the features of two dynamical diseases (CN in Colijn and Mackey, 2005a and PCML in Colijn and Mackey, 2005b), we chose it as a starting point in our quantitative investigation of CT. Extensive numerical experiments showed that any induced oscillations in the platelet compartment destabilize the neutrophil line. Our successive attempts lead to the conclusion that the hematopoietic model in this form cannot generate oscillatory solutions in platelet compartment while maintaining all the other variables at their steady state levels. The main cause of this phenomenon is the assumed dependence of the platelet differentiation rate on the number of circulating platelets. Since the molecular mechanisms of platelet regulation are not completely elucidated, given the similarities between erythropoiesis and thrombopoiesis, the authors assumed that the platelet differentiation rate follows the same mechanism as in the case of erythrocytes, and depends on the number of circulating cells. Searching the literature, we found that experimental data suggests that the megakaryocyte compartment is maintained by an approximately constant influx of progenitor cells (Branehog et al., 1975). Therefore, in our modeling work, we assume that the platelet differentiation rate is constant. For this reason, we will derive a new equation for the platelet dynamics and while maintaining the structure of the stem cell, neutrophil and erythrocyte compartments given in Colijn and Mackey (2005b) (see Fig. 1 for a cartoon representation). In the following, we present a brief model development, with a particular emphasis on the platelet compartment. The pluripotential, non-proliferating stem cells, the circulating neutrophils, platelets and erythrocytes are denoted by Q, N, P and R, respectively. We adopt the notation convention  $X_\tau(t) := X(t - \tau)$  for any variable  $X$ .

Table 1  
Inventory of the CT patients

Source and patient ID	Sex	Diagnosis	Mean of the data ( $\times 10^{10}$ cells/kg)	Significant period(s) (days)
Fogarty et al. (2005)	M	AI	1.7741	46
Rice et al. (2001)	F	AI&AM	0.1042	27
Kimura et al. (1996)	M	AI&AM	1.579	37 and 9
Helleberg (1995)	F	AI	0.9059	27
Kosugi et al. (1994)	F	AI	0.3290	25
Yanabu et al. (1993)	F	AI	1.9507	24
Rocha et al. (1991)	F	AI	1.0455	21 and 10
Menitove et al. (1989)	F	AI	1.1452	13
Skoog et al. (1957)	F	AI	0.5625	26
Bruin et al. (2005)	M	AM	0.6304	27
Füreder et al. (2002)	F	AM	1.7806	27
Zent et al. (1999)	M	AM	0.7267	30
Hoffman et al. (1989)	F	AM	1.1260	64
Aranda and Dorantes (1977)	M	AM	1.0984	29
Cohen and Cooney (1974)	F	AM	0.8064	30
Wilkinson and Firkin (1966)	M	AM	1.8701	41
Wasastjerna (1967)	M	AM	1.1354	23
Engstrom et al. (1966)	M	AM	1.7984	43
Von Schulthess and Gessner (1986), case 1	M	Healthy	1.9858	23
Von Schulthess and Gessner (1986), case 2	M	Healthy	2.9230	31 and 49
Morley (1969), subject 8	M	Healthy	1.7704	31
Lewis (1974)	F	C-TPO	0.9180	23

AI indicates autoimmune CT, AM denotes amegakaryocytic CT diagnosis, C-TPO stands for cycling TPO levels, and “healthy” are the asymptomatic patients.

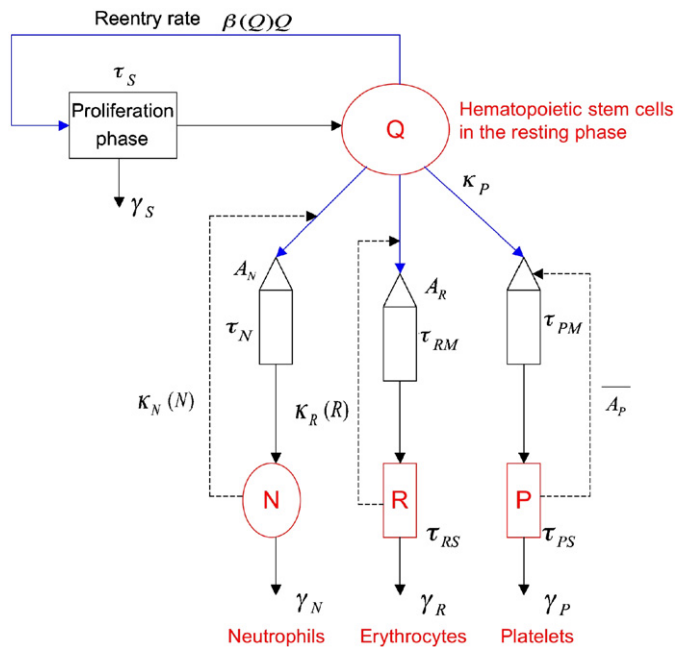


Fig. 1. The mathematic model of hematopoiesis. Solid arrows show the movement of cells, while dashed lines reflect the feedback functions.

### 3.1. Model development

#### 3.1.1. Stem cell compartment

The stem cells in the resting phase (or  $G_0$  phase) of the cell cycle do not divide. There are only two ways that they can exit

the non-proliferating compartment: either enter the proliferating phase at a rate  $\beta(Q)$  or differentiate into erythrocytes, neutrophils and platelets at rate  $\kappa_R$ ,  $\kappa_N$  and  $\kappa_P$ , respectively. After re-entering the proliferating phase, the cells divide, taking a time  $\tau_S$  to do so. Immediately after, the two daughter cells move into the resting phase. Using this notation, we can write a balance equation for the rate of change of HSC number as the difference between their production and their loss:

$$\frac{dQ}{dt} = \underbrace{-\beta(Q)Q}_{\text{movement into proliferation}} - \underbrace{(\kappa_N(N) + \kappa_P(P) + \kappa_R(R))Q}_{\text{loss due to differentiation}} + \underbrace{2e^{-\gamma_S\tau_S} \beta(Q_{\tau_S})Q_{\tau_S}}_{\text{cells reentering the } G_0 \text{ compartment}}$$

#### 3.1.2. Platelet compartment

Once a cell is committed to this pathway, it undergoes a series of nuclear divisions until it reaches the stage of megakaryocyte, which no longer proliferates but undergoes endoreduplication. A megakaryocyte needs  $\tau_{PM}$  days to mature and to release platelets into circulation. After  $\tau_{PS}$  days the platelets are primarily lost to senescence at a rate of  $\gamma_P$  per day. Colijn and Mackey (2005b) described the platelet variation by the following DDE:

$$\frac{dP}{dt} = -\gamma_P P + A_P \{ \kappa_P(P_{\tau_{PM}})Q_{\tau_{PM}} - e^{-\gamma_P\tau_{PS}} \kappa_P(P_{\tau_{PM}+\tau_{PS}})Q_{\tau_{PM}+\tau_{PS}} \},$$

where the platelet differentiation rate  $\kappa_P$  is given by

$$\kappa_P(P) = \frac{\bar{\kappa}_r}{1 + K_P P^r}.$$

In our work, we assume that the platelet differentiation rate is constant, and we use

$$\frac{dP}{dt} = -\gamma_P P + \bar{A}_P \kappa_P(Q_{\tau_{PM}} - e^{-\gamma_P \tau_{PS}} Q_{\tau_{PM} + \tau_{PS}}). \quad (3)$$

to model the platelet dynamics. The main agent controlling the peripheral platelet regulatory system through  $\bar{A}_P$  (the average number of platelets released per megakaryocyte) is TPO. Let  $V(t)$  denote the megakaryocyte volume and  $T(t)$  the TPO concentration at the time  $t$ . The available experimental data suggests that

- (i)  $\bar{A}_P(t) \propto V(t)$  and
- (ii)  $V(t)$  obeys the ordinary differential equation  $\frac{dV}{dt}(t) = \mu T(t)V(t)$ .

From this we obtain:

$$V(t) = V(t - \tau_{PM}) e^{\mu \int_{t-\tau_{PM}}^t T(t') dt'}.$$

Since the differentiation rate  $\kappa_P$  is constant we can consider  $V(t - \tau_{PM}) = V_0$ . Hence

$$\bar{A}_P(t) = A_0 e^{\mu \int_{t-\tau_{PM}}^t T(t') dt'},$$

where  $A_0$  denotes the minimal number of platelets produced per megakaryocyte. Note that

$$\bar{T}(t) := \frac{1}{\tau_{PM}} \int_{t-\tau_{PM}}^t T(t') dt'$$

represents the average TPO concentration at the time  $t$ . Hence

$$\bar{A}_P(t) = A_0 e^{\mu \tau_{PM} \bar{T}(t)}.$$

Santillán et al. (2000) model the TPO concentration under the assumption that the number of megakaryocytes of age zero entering from the stem cell compartment is directly proportional to the TPO levels. They find

$$\frac{dT}{dt} = \frac{a}{1 + K_P P^r} - \kappa T.$$

Additionally, if we consider that TPO concentration is in dynamic equilibrium with the number of circulating platelets then  $\frac{dT}{dt} = 0$ . Therefore

$$T \propto \frac{1}{1 + K_P P^r}, \quad \text{which implies} \quad T = \frac{T_{max}}{1 + K_P P^r}.$$

$T_{max}$  represents the maximum TPO level in blood.

### 3.1.3. Erythrocyte compartment

The erythrocyte and platelet dynamics share common features and display some important differences. The primary difference between erythropoiesis and thrombopoiesis is

related to the development of the precursor cells. In erythropoiesis, the stem cells undergo rapid proliferation and differentiation until they become reticulocyte, which mature and become circulating erythrocytes. Therefore the total variation of erythrocytes is described by

$$\begin{aligned} \frac{dR}{dt} = & \underbrace{-\gamma_R R}_{\text{random loss}} + \underbrace{A_R \kappa_R(R_{\tau_{RM}}) Q_{\tau_{RM}}}_{\text{cells entering from the stem cell compartment}} \\ & - \underbrace{A_R e^{-\gamma_R \tau_{RS}} \kappa_R(R_{\tau_{RM} + \tau_{RS}}) Q_{\tau_{RM} + \tau_{RS}}}_{\text{loss due to senescence}}. \end{aligned}$$

All the notation (except for  $A_R$ ) is analogous to that in Eq. (3).  $A_R$  is a dimensionless parameter corresponding to the amplification stage due to cell division.

### 3.1.4. Neutrophil compartment

As the neutrophil precursors differentiate, their number is amplified by a constant factor  $A_N$  which accounts for the stages of cell division. After  $\tau_N$  days they become mature and are released into circulation. The neutrophils are randomly lost at the rate  $\gamma_N$ . Their dynamics is governed by the equation:

$$\frac{dN}{dt} = \underbrace{-\gamma_N N}_{\text{random loss}} + \underbrace{A_N \kappa_N(N_{\tau_N}) Q_{\tau_N}}_{\text{cells entering from the stem cell compartment}}.$$

We adopt the same form of the negative feedback functions for the erythrocyte ( $\kappa_R(R)$ ) and neutrophil ( $\kappa_N(N)$ ) compartments, as well as the form of the stem cell reentry rate ( $\beta(Q)$ ) as in Colijn and Mackey (2005b). They are the result of the previous modeling work (Bernard et al., 2003; Mahaffy et al., 1998; Mackey, 1979) and are consistent with the physiological framework.

Summarizing, the equations comprising the model are:

$$\begin{cases} \frac{dQ}{dt} = -(\beta(Q) + \kappa_N(N) + \kappa_P + \kappa_R(R))Q \\ \quad + 2e^{-\gamma_S \tau_S} \beta(Q_{\tau_S}) Q_{\tau_S}, \\ \frac{dN}{dt} = -\gamma_N N + A_N \kappa_N(N_{\tau_N}) Q_{\tau_N}, \\ \frac{dR}{dt} = -\gamma_R R + A_R (\kappa_R(R_{\tau_{RM}}) Q_{\tau_{RM}} \\ \quad - e^{-\gamma_R \tau_{RS}} \kappa_R(R_{\tau_{RM} + \tau_{RS}}) Q_{\tau_{RM} + \tau_{RS}}), \\ \frac{dP}{dt} = -\gamma_P P + \bar{A}_P \kappa_P(Q_{\tau_{PM}} - e^{-\gamma_P \tau_{PS}} Q_{\tau_{PM} + \tau_{PS}}), \end{cases} \quad (4)$$

where

$$\begin{aligned} \beta(Q) &= k_0 \frac{\theta_2^s}{\theta_2^s + Q^s}, & T &= \frac{T_{max}}{1 + K_P P^r}, \\ \kappa_N(N) &= f_0 \frac{\theta_1^n}{\theta_1^n + N^n}, & \bar{A}_P(t) &= A_0 e^{\mu \tau_{PM} \bar{T}(t)}, \\ \kappa_R(R) &= \frac{\bar{\kappa}_r}{1 + K_r R^m}, & \bar{T}(t) &= \frac{1}{\tau_{PM}} \int_{t-\tau_{PM}}^t T(t') dt'. \end{aligned}$$

### 3.2. Parameter estimation

The parameter estimation is one of the most important aspects of our modeling work since the biologically relevant choice of the parameters is crucial to establish the onset of oscillations observed in CT. Using experimental data published in the literature we evaluate all the parameters outside the negative feedback functions. Bernard et al. (2003) derived all the values corresponding to the stem cell and leukocyte compartments. We use their evaluations except for the dimensionless amplification parameter  $A_N$  and the Hill coefficient  $f_0$ .  $A_N$  has been estimated by Mackey (2001) as 300,000 and we use this value. The normal range for  $f_0$  is 0.4 – 1.5 (Bernard et al., 2003). Bernard et al. (2003) chose  $f_0 = 0.8$  to make the model fit the data. Since our model estimates

$$f_0 = \kappa(N_*) \frac{\theta_1 + N_*}{\theta_1} = \frac{\gamma_N N_*}{A_N Q_*} \times \frac{\theta_1 + N_*}{\theta_1} = 0.4,$$

we set  $f_0 = 0.4$ .

The erythrocyte parameters are evaluated by Mahaffy et al. (1998) based on experimental human data. To their estimates we add the dimensionless amplification parameter  $A_R = 563,000$  (Beutler et al., 1995; Colijn and Mackey, 2005b), and the Hill coefficient  $\bar{\kappa}_r$  estimated in Colijn and Mackey, 2005b as  $1.1 \text{ days}^{-1}$ .

Santillán et al. (2000) give the normal values of  $\gamma_P$ ,  $\tau_{PM}$ ,  $\tau_{PS}$  and the mean platelet count  $P_* = 2.5 \times 10^8 \text{ cells/ml}$ . Using the fact that 70 kg adult has 6 L of blood (Colijn and Mackey, 2005b) we find  $P_* = 2.14 \times 10^{10} \text{ cells/kg}$ . For the platelet control dynamics we need to estimate the effective growth rate of megakaryocytes ( $\mu$ ), the minimum number of platelets produced per megakaryocyte ( $A_0$ ), the differentiation rate ( $\kappa_P$ ), and the maximum TPO concentration ( $T_{max}$ ). Experimental measurements show that one mature megakaryocyte can give rise to 1000–5000 platelets (Beutler et al., 1995). Therefore we choose  $A_0 = 1000$  platelets per megakaryocyte. By fitting the TPO concentrations versus the platelet count, Santillán et al. (2000) evaluate

$$T_* = 0.005 \text{ U/ml}, \quad T_{max} = 32.18 T_*, \quad K_P = \frac{31.18}{(P_*)^r},$$

and  $r = 1.29$ .

Converting to cells/kg we obtain

$$T_* = 0.428 \text{ U/kg}, \quad T_{max} = 13.773 \text{ U/kg}$$

and  $K_P = 11.66 \times (10^{10} \text{ cells/kg})^{-r}$ .

Deriving the model parameters we have to make sure that there is a balance between the influx and the efflux from the resting phase of the stem cell compartment. Mathematically, this means that at steady state the following relation should be satisfied

$$-(\kappa_R^* + \kappa_N^* + \kappa_P) + 2e^{-\gamma_S \tau_S} \beta_* = 0.$$

The above equation determines the normal value of the platelet differentiation rate:

$$\kappa_P = (2e^{-\gamma_S \tau_S} - 1)\beta_* - \kappa_R^* - \kappa_N^* = 0.028 \text{ days}^{-1}.$$

Once all the other parameters are estimated, it is easy to evaluate the effective growth rate of megakaryocytes:

$$\begin{aligned} \mu &= \frac{1}{T_* \tau_{PM}} \ln \frac{\overline{A_P}^*}{A_0} = \frac{1}{T_* \tau_{PM}} \ln \frac{\gamma_P P_*}{\kappa_P A_0 Q_* (1 - e^{-\gamma_P \tau_{PS}})} \\ &= 1.7836 \text{ (U days/kg)}^{-1}. \end{aligned}$$

### 4. Simulating CT

First, we want to understand the model dynamics by looking at the influence of each parameter on the stability of the steady state, and by analyzing the changes in the amplitude and the period of oscillations once stability is lost. Periodic hematological diseases like PCML and CN, which involve fluctuations in all blood cell lines, are believed to arise in the stem cell compartment in the bone marrow. Since all the reported cases of CT, except for Füreder et al. (2002) and Menitove et al. (1989), reveal that besides oscillations in platelet count the patient's hematological profile has been consistently normal, a destabilization of a peripheral control mechanism might play an important role in the genesis of this disorder. For this reason we confine our numerical investigation to the set of parameters which generate periodic solutions in the platelet compartment and held all the other model variables at their normal values. The next step of our investigation is to fit the simulated data provided by the model to the published platelet counts.

#### 4.1. Model dynamics

Initially, we tried numerical experiments based on the existing notions of the mechanisms of CT. The literature up to now explains the aetiology of this disease in terms of platelet destruction (autoimmune CT) or cyclical failure in platelet production (amegakaryocytic CT). Spectral data analysis revealed that an important feature of CT is the significant periods of platelet fluctuations. They vary between individuals and are in the range 13–64 days. First, we increased the death rate of circulating platelets  $\gamma_P$  to determine whether this change induces oscillations like those seen in autoimmune data. Although the model displays a highly sensitive response to small changes in  $\gamma_P$  and the platelet counts start immediately to oscillate, the period of fluctuations remains unchanged ( $\approx 13$  days). It is of interest to discover how the mathematical model can generate oscillatory solutions with different periodicity. Repeated numerical integrations show that the main parameter controlling the period of platelet fluctuations is the maturation time of megakaryocytes  $\tau_{PM}$ . Fig. 2 captures the period evolution when  $\tau_{PM}$  is varied over a

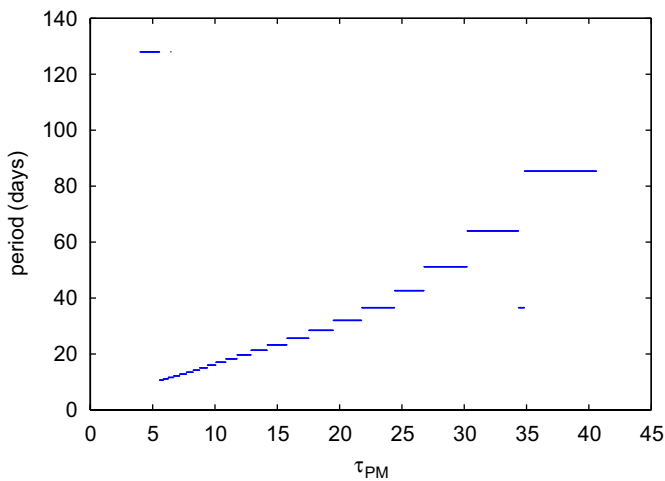


Fig. 2. Evolution of periodicity in platelet oscillations when the maturation time of megakaryocytes  $\tau_{PM}$  is modified.

large range. As it is illustrated in Fig. 3, changes in  $\gamma_p$  or  $\mu$  do not significantly affect the period of platelet oscillations. Based on the hypothesis that the cyclical patterns in amegakaryocytic CT are secondary to the failure in platelet production, we decreased the platelet differentiation rate  $\kappa_P$  from its steady state value to much lower levels. This change did not lead to a bifurcation in the stability of the steady state, with sustained oscillations in the platelet compartment.

CT involves either thrombocytosis (high platelet count), thrombocytopenia (low platelet values) or an alternation of both. One way to simulate the low/high platelet levels is by decreasing/increasing the minimal number of platelets released per megakaryocyte ( $A_0$ ) and the effective growth rate of megakaryocytes ( $\mu$ ).

The above discussion identifies a subset in the parameter space with an essential role in generating a model response similar with the CT platelet data: the platelet apoptosis rate ( $\gamma_P$ ), the effective growth rate of megakaryocytes ( $\mu$ ), the minimal number of platelets released per megakaryocyte ( $A_0$ ), and the megakaryocytes maturation time ( $\tau_{PM}$ ). None of the changes in the values of these four parameters perturb the stem cells, erythrocytes or neutrophils normal levels.

#### 4.2. Fitting the model simulations to platelet data

To our knowledge, simulated annealing is one of the most successful techniques for large scale optimization problems where the global minimum is hidden between many local extrema. It was introduced by Kirkpatrick et al. (1983) and it is inspired by the slow cooling of the liquid metals (annealing). The algorithm works by simulating a random walk on the set of the configuration space that searches for low energy states. At each instant during the simulation we have a current state from which we randomly select a neighbor and consider probabilistically whether to move at the new configuration and try again.

The great advantage of this technique is that the system cannot be trapped in a local minimum. Inspired by the physical processes, Kirkpatrick et al. (1983) introduce a global temperature parameter  $\mathcal{T}$  to control the cooling rate of the system. If none of the moves tested decrease the energy, then an uphill move is accepted with probability  $P = e^{-\Delta E/\mathcal{T}}$ .  $\Delta E$  denotes the difference between the new and the old values of the energy function  $E$ .

For our optimization problem we choose as an energy function the square root of the pointwise least square between the clinical data and simulated platelet data:

$$E = \sqrt{\sum_{i=1}^M \frac{(P_i^s - P_i)^2}{\bar{P}^2}}$$

$M$  is the number of points available, the presence/lack of the superscript  $s$  indicates simulated/CT data. The square root and the mean of the CT data  $\bar{P}$  are introduced for technical reasons. The square root deforms the function monotonically, making the energy landscape less steep and  $\bar{P}$  provides scaling information. The success of the algorithm depends on the sequence of decreasing temperatures (the annealing schedule). This schedule is not unique and it is challenging to find the appropriate one for each problem. Initially, we tried a geometric schedule, i.e.  $\mathcal{T}(t+1) = \alpha\mathcal{T}(t)$ , with  $\alpha$  very close to 1 ( $\alpha = 0.999$ ), but it was not slow enough to find the “optimum” configuration. Although not very common, the constant thermodynamic speed schedule allowed sufficient time for finding the minimum energy state:

$$\Delta\mathcal{T} = -\frac{v\mathcal{T}^2}{\varepsilon\sigma(E)},$$

where  $\Delta\mathcal{T}$  is the difference between the current and the previous temperature,  $\sigma(E)$  represents the standard deviation of the current energy,  $\varepsilon$  is the estimate of the relaxation time, and  $v$  is the thermodynamic speed (constant). The Matlab implementation of this method was constructed in the framework offered by Press et al. (1993) and Salamon et al. (2002). The delay differential equations comprising the model (4) are numerically integrated using a Runge–Kutta method (time step 0.05 days) incorporated in the mathematical software XPP (Ermentrout, 2002). The initial conditions are the steady state values from Table 2 and approximately 200 days are discarded to eliminate transient behavior.

##### 4.2.1. Fitting results

We applied this approach to the CT data, comparing the model simulation to the platelet counts published in the literature. By varying the parameters  $\gamma_P$ ,  $\mu$ ,  $\tau_{PM}$ ,  $A_0$ , and, in some isolated cases,  $\kappa_P$  and  $\theta_2$ , we were able to successfully duplicate the dynamic clinical features of CT. The simulated annealing output and platelet data recorded from the patients diagnosed with CT are



Table 2  
Estimated equilibrium values for normal subjects

Parameter name	Value used	Unit	Source
<i>Stem cell compartment</i>			
$Q_*$	1.1	$10^6$ cells/kg	1
$\gamma_S$	0.07	days <sup>-1</sup>	1
$\tau_S$	2.8	days	1
$k_0$	8.0	days <sup>-1</sup>	1
$\theta_2$	0.095	$10^6$ cells/kg	1
$s$	2	(none)	1
<i>Neutrophil compartment</i>			
$N_*$	6.9	$10^8$ cells/kg	1, 3
$\gamma_N$	2.4	days <sup>-1</sup>	1, 3
$\tau_N$	3.5	days	1, 3
$A_N$	$3000 \times 10^2$	(none)	4
$f_0$	0.40	days <sup>-1</sup>	3
$\theta_1$	0.36	$10^8$ cells/kg	1, 3
$n$	1	(none)	1, 3
<i>Erythrocyte compartment</i>			
$R_*$	3.5	$10^{11}$ cells/kg	5, 3
$\gamma_R$	0.001	days <sup>-1</sup>	5, 3
$\tau_{RM}$	6	days	5, 3
$\tau_{RS}$	120	days	5, 3
$A_R$	$5.63 \times 10^5$	(none)	2, 3
$\bar{\kappa}_r$	0.5	days <sup>-1</sup>	3
$K_r$	0.0382	$(10^{11}$ cells/kg) <sup>-m</sup>	5, 3
$m$	6.96	(none)	5, 3
<i>Platelet compartment</i>			
$P_*$	2.14	$10^{10}$ cells/kg	6, 3
$\gamma_P$	0.15	days <sup>-1</sup>	6, 3
$\tau_{PM}$	7	days	6, 3
$\tau_{PS}$	9.5	days	6, 3
$\mu$	1.7836	(U days/kg) <sup>-1</sup>	Calculated
$A_0$	$0.1 \times 10^4$	$10^4$	2
$\kappa_P$	0.028	days <sup>-1</sup>	Calculated
$K_P$	11.68	$(10^{10}$ cells/kg) <sup>-r</sup>	3, 6
$r$	1.29	(none)	3, 6
$T_*$	0.428	U/kg	6
$T_{max}$	13.773	U/ kg	Calculated

Sources: 1 = Bernard et al. (2003), 2 = Beutler et al. (1995), 3 = Colijn and Mackey (2005b), 4 = Mackey (2001), 5 = Mahaffy et al. (1998), 6 = Santillán et al. (2000).

presented in Appendix B (see Figs. B1, B2). The left-hand panels contain the sampled simulation (model output sampled at the same time points as the clinical data) and the right-hand column shows the full platelet simulation generated by our model. Since the available experimental results associate autoimmune CT to an immune-mediated platelet destruction, we would expect that an increase in the rate of platelet clearance ( $\gamma_P$ ) would be the primary change necessary for duplicating some cases of CT. Indeed,  $\gamma_P$  appears to be involved in fitting autoimmune data as well as in few amegakaryocytic situations, with significantly increased values in the first variety of the disease (average 0.3 with a standard deviation of 0.09) comparable to the latter (average 0.19 with a standard deviation of 0.01).

The platelet differentiation rate ( $\kappa_P$ ), the minimal number of platelets released per megakaryocyte ( $A_0$ ), and the relative growth rate of megakaryocyte ( $\mu$ ) were changed while fitting the model to platelet data, as it was hypothesized that amegakaryocytic CT involves a megakaryocyte deficiency and a cyclical failure in platelet production. Repeated numerical experiments indicate that there is no significant advantage varying  $\kappa_P$ . In all cases but one (Zent et al., 1999), the fitting algorithm did not modify this parameter. Surprisingly, for the patient reported by Zent et al. (1999) a stem cell parameter change was necessary for fitting. Although it was sufficient to change  $\tau_{PM}$ ,  $\mu$ , and  $\kappa_P$  to the numerical values from Table 3 to mimic the platelet counts of this patient, stem cell levels increased to approximately  $2.2 \times 10^6$  cells/kg. When reducing  $\theta_2$  at about half of its normal value, stem cells returned to the equilibrium, while the platelet counts remained unchanged. In the simulated annealing results, the values of  $\mu$  are drastically reduced relative to the normal value of  $1.7839$  (U days/kg)<sup>-1</sup>.  $\mu$  varied between  $\frac{1}{45}$  and  $\frac{1}{10}$  of the steady state value which is physiologically equivalent to a slower relative growth of megakaryocytes in all CT patients investigated in our study. These findings are in agreement with the clinical features of CT. Bruin et al. (2005) and Zent et al. (1999) described amegakaryocytic patients with small megakaryocytes in the ascending limb of the platelet count cycle.

Only in a few cases was it necessary to decrease  $A_0$  to simulate CT. Generally, this parameter was reduced to either half or  $\frac{1}{10}$  of its normal value. Interestingly, in a single case of amegakaryocytic CT (Bruin et al., 2005)  $A_0$  was decreased by a factor of 200 compared to the steady state value. This is consistent with the clinical observations, since bone marrow aspirates in this patient showed small megakaryocytes with no release of platelets (Bruin et al., 2005).

Since the period of platelet fluctuations in CT data varies between individuals, and  $\tau_{PM}$  (megakaryocyte maturation time) is the parameter with the most prominent influence on the platelet oscillations generated by the model, we allowed  $\tau_{PM}$  to vary. What was not anticipated in this study is the major role played by  $\tau_{PM}$  in reproducing the oscillatory patterns observed in CT. Furuyama et al. (1999) presented an autoimmune case where the megakaryocytes are always abundant, but most of them are immature at platelet nadir and only 50% are mature at the time of high platelet count. Also, Aranda and Dorantes (1977) noticed that in their patient CT was related to a periodic variation in maturity of megakaryocytes. Our results indicate that megakaryocytes need about twice as much time as normal to mature in autoimmune CT. In the patients with amegakaryocytic CT, which have on average longer periods of platelet fluctuations,  $\tau_{PM}$  is elevated between two and six times the normal value.

#### 4.2.2. TPO levels in CT patients

Since TPO is the primary regulator of platelet production, abnormalities of this hormone or its receptor might be

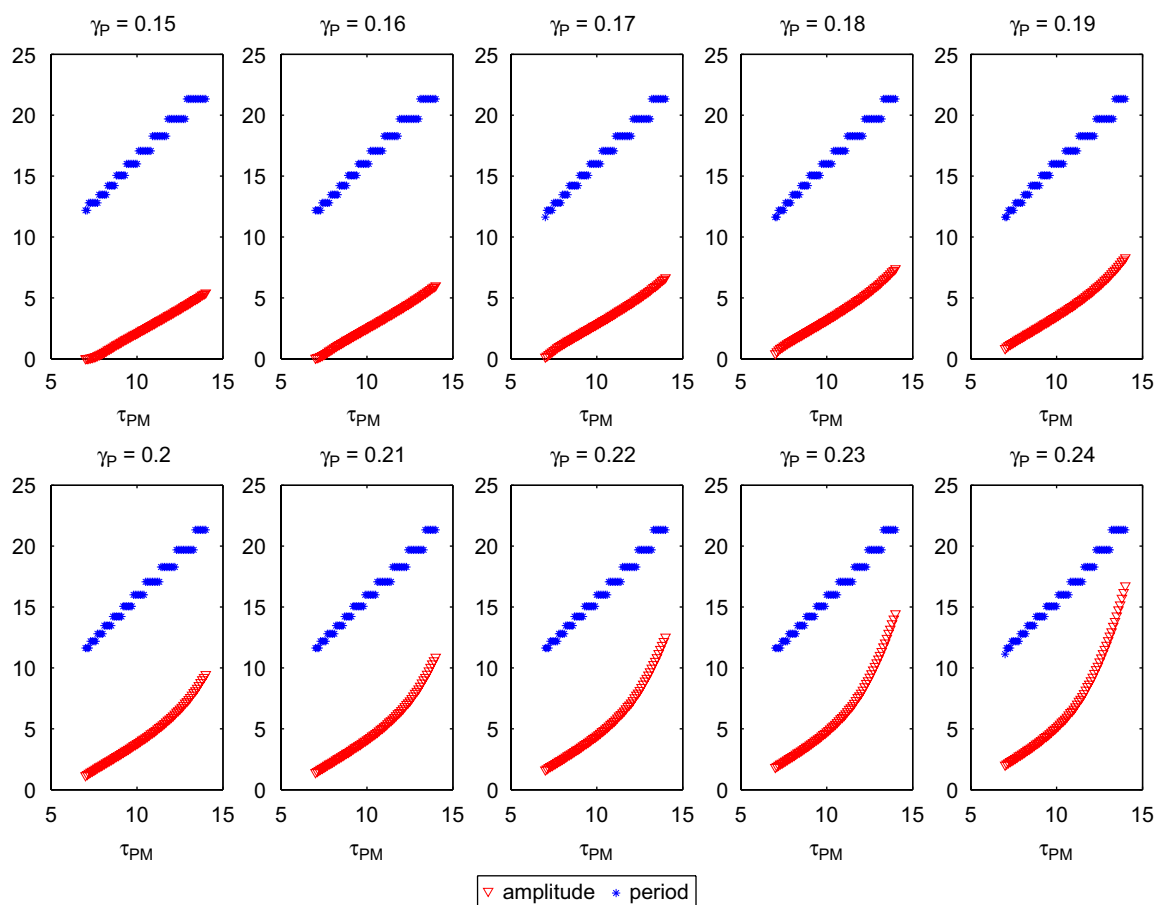


Fig. 3. Changes in the period (days) and the amplitude ( $\times 10^{10}$  cells/kg) of platelet fluctuations when  $\gamma_P$  and  $\tau_{PM}$  are varied simultaneously. All the other parameters are kept at their normal values (see Table 2). A small increase in  $\gamma_P$  determines an oscillatory response with an increased amplitude but unchanged period. Similarly, perturbations in  $\tau_{PM}$  values induce platelet oscillations with variable period and unchanged amplitude.

Table 3  
Parameter estimates for the CT patients based on simulated annealing method

Source and patient ID	$\gamma_P$	$\tau_{PM}$	$\mu$	$A_0$	$\theta_2$	$\kappa_P$	Transient	CV
Normal values (NV)	0.15	7	1.7836	0.1	0.095	0.028		
<i>Autoimmune CT</i>								
Kosugi et al.	0.40317	16.995	0.044527	0.056734	NV	NV	200	0.6710
Yanabu et al.	0.2738	17.001	0.23746	NV	NV	NV	212	0.7098
Rocha et al.	0.35764	14.0086	0.16654	NV	NV	NV	200	0.6398
Kimura et al.	0.2	26	0.17836	NV	NV	NV	216	0.8346
Skoog et al.	0.21923	20.0024	0.17913	0.016788	NV	NV	203.5	0.8871
<i>Amegakaryocytic CT</i>								
Bruin et al.	NV	16.598	0.200644	0.00050384	NV	NV	215	0.9570
Zent et al.	NV	19.656	0.1482	NV	0.05435	0.002332	198	0.9748
Hoffman et al.	NV	40.044	0.048642	NV	NV	NV	205	0.7735
Wilkinson & Firkin	0.09319	27.843	0.1595	NV	NV	NV	205	0.7248
Engstrom et al.	0.19614	27.4434	0.17548	NV	NV	NV	205	0.9120
Aranda & Dorantes	0.20632	19.297	0.15719	NV	NV	NV	218	0.4243
Wasastjerna	0.39526	16.374	0.17911	NV	NV	NV	222	0.8254
<i>C-TPO</i>								
Lewis	0.22	18	0.17836	0.01	NV	NV	215	0.9228

NV stands for the normal value taken from Table 2. CV denotes the coefficient of variation between the clinical data and our simulations.

responsible for platelet fluctuations. Some research groups (Bruin et al., 2005; Kimura et al., 1996; Rice et al., 2001; Zent et al., 1999) measured the platelet counts in CT patients as well as the temporal evolution of TPO concentration. For these patients, the same parameter changes generated a very

good fit of the platelet counts and an encouraging qualitative comparison of the predicted and the published TPO levels (Fig. 4). This supports the accuracy of our model predictions and suggests that the TPO oscillations are secondary manifestations of some other pathology.

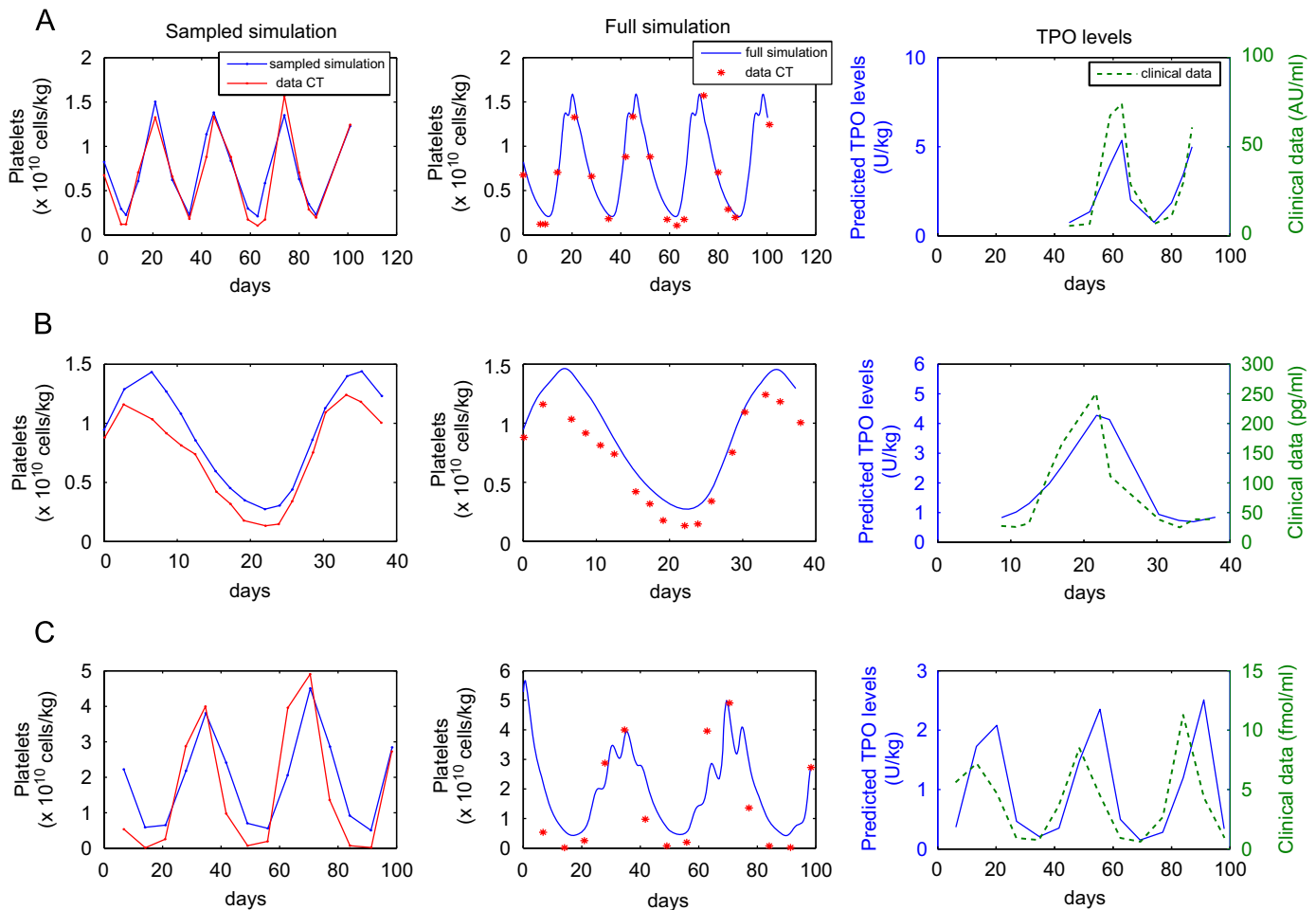


Fig. 4. With the same parameter changes, the model is able to fit the platelet counts and to qualitatively reproduce the TPO oscillations. (A) Bruin et al. (2005), (B) Zent et al. (1999), (C) Kimura et al. (1996).

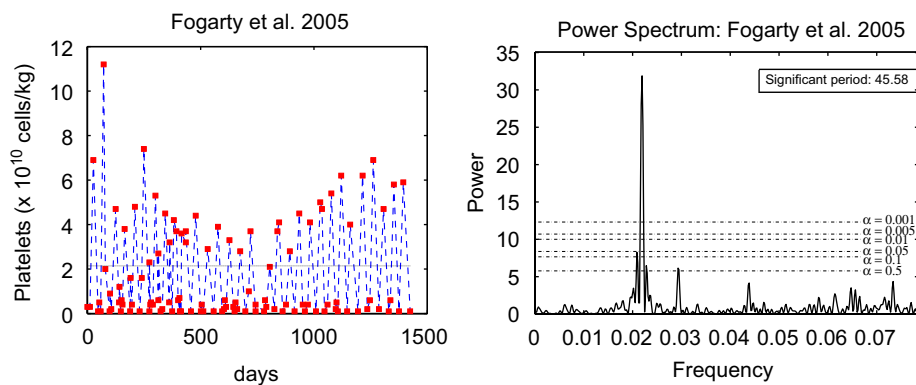


Fig. A1. *Left-hand panels:* Published platelet counts of a patient diagnosed with autoimmune CT. The horizontal line shows the normal platelet value in humans ( $2.14 \times 10^{10}$  cells/kg). *Right-hand panels:* The corresponding periodogram (power versus frequency). The horizontal lines specify the significance levels.

### 5. Hypothesis for the origin of oscillations in CT

A variety of modeling studies (Bélair and Mackey, 1987; Bélair et al., 1995; Bernard et al., 2003; Colijn and Mackey, 2005a, b, 2007; Mahaffy et al., 1998; Pujol-Menjouet et al., 2005; Santillán et al., 2000) have associated the onset of

oscillations in hematological disease with a Hopf bifurcation induced by the change of one or more physiological parameters. Though the model we have developed here was too complicated for a complete stability analysis (Apostu, 2007) we hypothesize that the oscillations seen in CT and studied here are also due to a Hopf bifurcation.

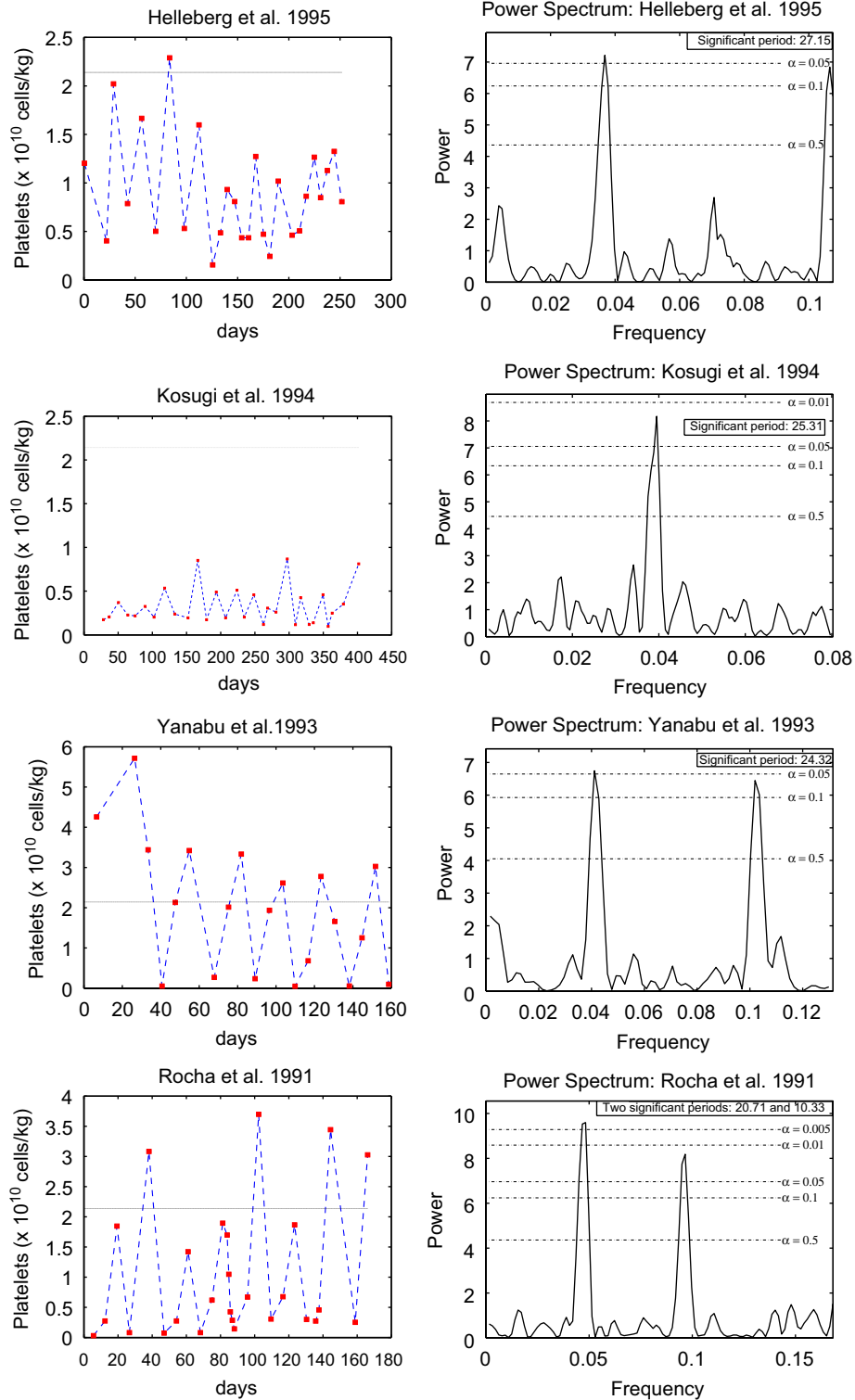


Fig. A2. Published platelet counts of patients diagnosed with autoimmune CT. All the other notation as in Fig. A1.

The mathematical model (4) successfully duplicated both the qualitative and quantitative features of CT. The high values of the coefficient of variation between the clinical data and the model simulations lend credibility to our hypothesis (See Table 3). The platelet fluctuations in amegakaryocytic

CT are caused by a cyclic inhibition of megakaryocytopoiesis, accentuated by an increased platelet maturation time and a reduced release of platelets per megakaryocyte. The critical parameter changes required to mimic the corresponding data are a severe decrease in  $\mu$ , an increase in  $\tau_{PM}$  between 2 and 6

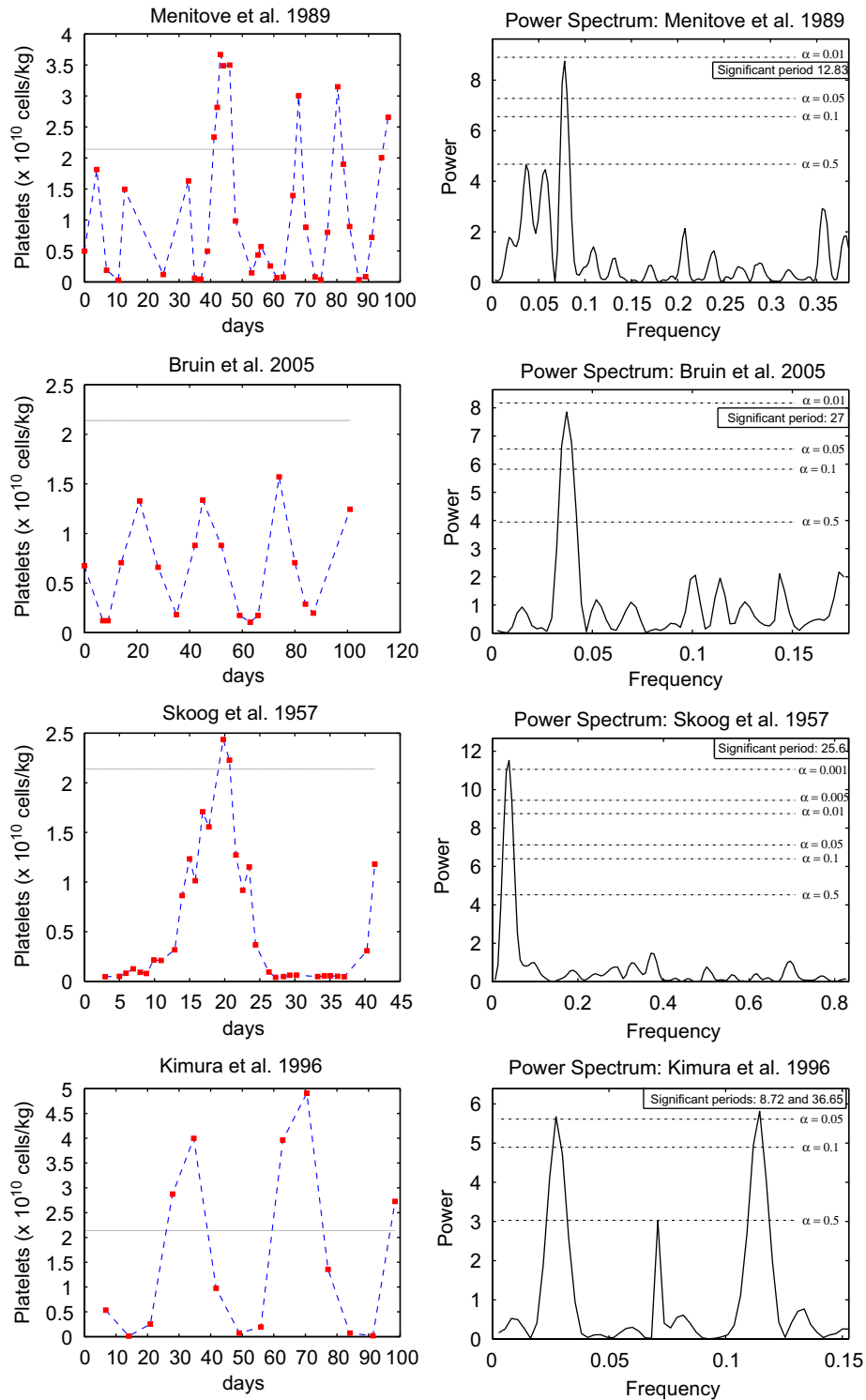


Fig. A3. Published platelet counts of patients diagnosed with autoimmune CT (Menitove et al., 1989) or amegakaryocytic CT (all the others). All the other notation as in Fig. A1.

times the normal value, and occasionally, a reduced  $A_0$ . In the case of autoimmune CT, the most significant parameter changes recorded during the successful attempts to fit the autoimmune data are an elevation of  $\gamma_P$ , a decrease of  $\mu$ , and an increase in  $\tau_{PM}$  by a factor of 2. These results suggest that the onset of oscillations in autoimmune CT can be explained by an accelerated peripheral destruction of platelets, exacerbated by an increased maturation of megakaryocytes and a slow relative growth rate of megakaryocytes.

bated by an increased maturation of megakaryocytes and a slow relative growth rate of megakaryocytes.

## 6. Discussion and conclusion

For many years the pathogenesis of CT was not clearly understood and up to now it remains speculative. Clinical

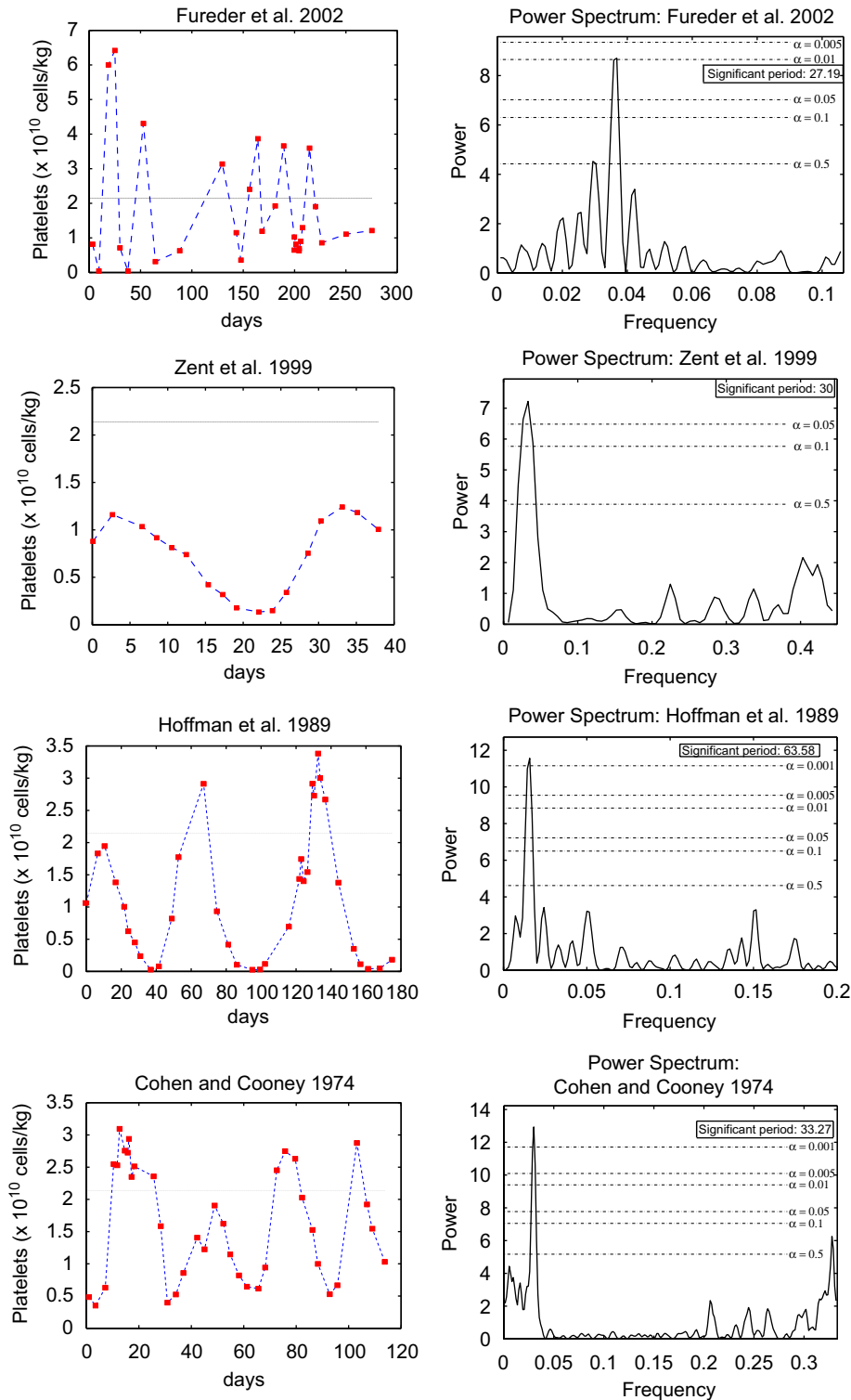


Fig. A4. Published platelet counts of patients diagnosed with amegakaryocytic CT. All the other notation as in Fig. A1.

attempts to explain the aetiology of platelet fluctuations led to different conclusions. Generally, the onset of oscillations was explained in terms of immune-mediated platelet destruction or periodic failure of platelet production. To our knowledge, only two modeling studies have been directed at the investigation of CT. Von Schulthess and

Gessner (1986) suggested that, in the case of their asymptomatic patients, the platelet control was biased close to a stability boundary (Swinburne and Mackey, 2000; Von Schulthess and Gessner, 1986). The second modeling effort is that of Santillán et al. (2000). They formulated an age-structured model for the regulation of

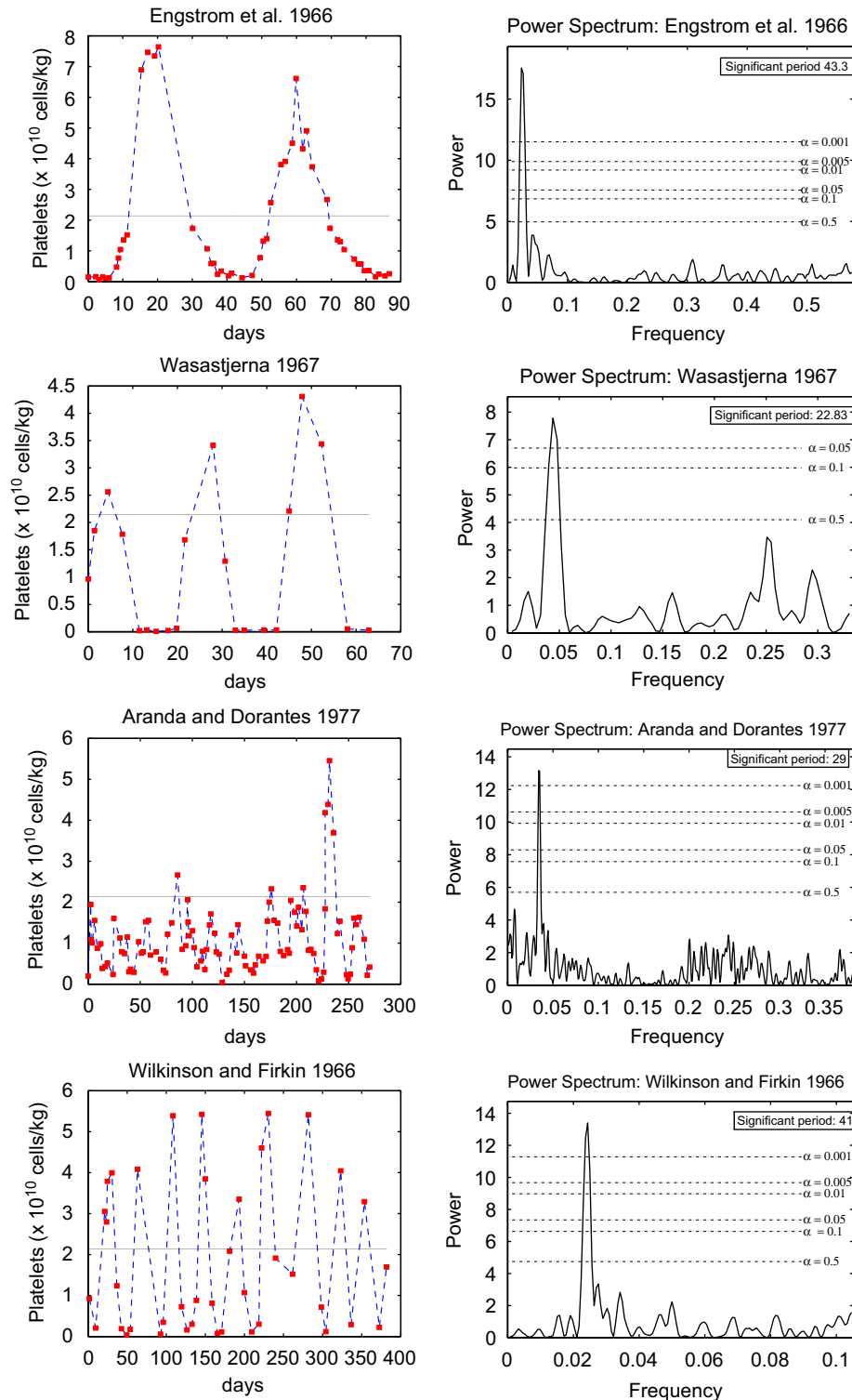


Fig. A5. Published platelet counts of patients diagnosed with amegakaryocytic CT. All the other notation as in Fig. A1.

the platelet production which reproduced the features of autoimmune CT. Their work suggests that autoimmune and amegakaryocytic CT have a different dynamical origin

and that the platelet oscillations in autoimmune CT are due to a supercritical Hopf bifurcation induced by an increased death rate of the circulating platelets.

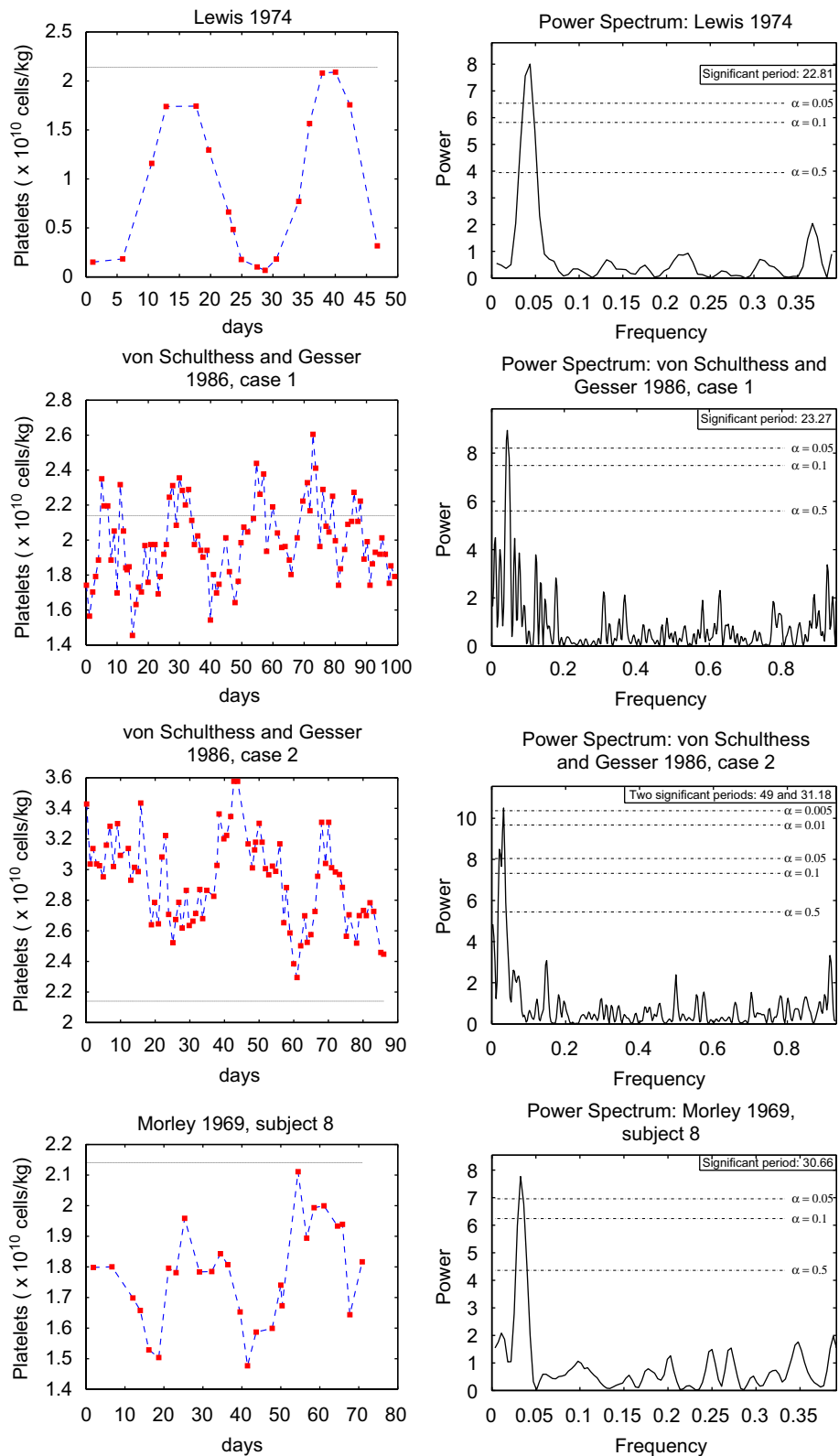


Fig. A6. Published platelet counts of asymptomatic patients diagnosed with CT. All the other notation as in Fig. A1.



The mathematical model (4) proposed in this paper is in agreement with the biological framework, successfully duplicates the platelet counts of CT patients, and provides a qualitative fitting of the thrombopoietin levels (when data is available). The results of our investigation agree with the clinical findings, explain the experimental observations, partially support the conclusions drawn from the previous modeling effort, and suggest new factors responsible for the fluctuating pattern in platelets. Since autoimmune and amegakaryocytic CT share common features and display important differences, we would expect a common nucleus in the mechanisms generating these two varieties. Indeed, our model reveals that in general, changes in the megakaryocyte maturity ( $\tau_{PM}$ ), the relative growth rate of megakaryocytes ( $\mu$ ), the minimal number of platelets released per megakaryocyte ( $A_0$ ) and the random destruction of platelets ( $\gamma_P$ ) are necessary to reproduce the clinical data, but the range where these parameters vary depends on the type of CT. As in amegakaryocytic CT, in autoimmune CT the rate of platelet clearance is higher, the megakaryocytes spend less time in the bone marrow, and their relative growth rate is closer to the normal value. Based on the laboratory results, it was previously believed that platelet fluctuations in autoimmune CT are secondary to an elevated platelet destruction. The numerical experiments performed with our model show that only increasing  $\gamma_P$  is not sufficient to reproduce the platelet data of the autoimmune patients and that other factors also contribute to the disease. In simulating amegakaryocytic CT and autoimmune CT more than one parameter had to be modified to reproduce the hematological data and, in our opinion, this fact implies multiple physiological causes. We believe that both types of CT are due to a Hopf bifurcation in the platelet dynamics, but the parameter change inducing the bifurcation depends on the type of cyclical thrombocytopenia.

### Acknowledgments

This work was supported by Mathematics of Information Technology and Complex Systems (MITACS), Canada and Natural Sciences and Engineering Research Council of Canada (NSERC). We would like to thank Dr. Moisés Santillán for helpful suggestions in modeling the platelet dynamics.

### Appendix A. Data analysis: time series and Lomb–Scargle periodograms

The platelet data collected from the literature is presented either as cells/L or as cells/kg. In our study, we maintain the same unit (cells/kg) using for conversion the fact that 70 kg adult has 6 L blood (Colijn and Mackey, 2005b). As we mentioned before, all the platelet counts are tested for the statistically significant periodicity using

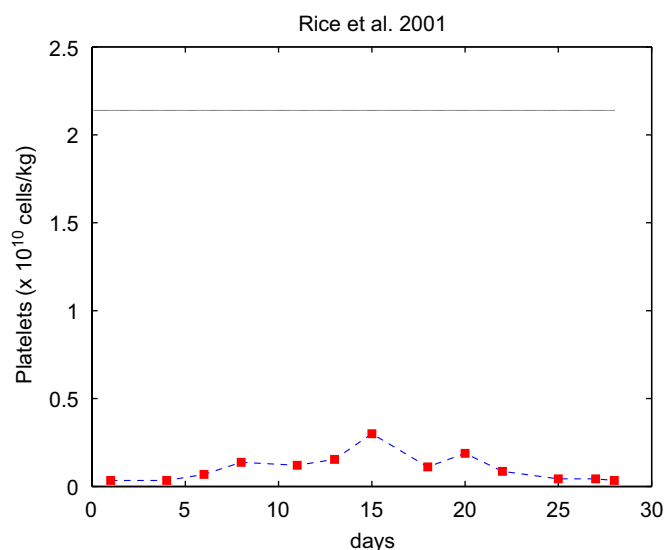


Fig. A7. The patient reported by Rice et al. (2001) was responsive to thrombopoietic growth factor therapy. In our investigation we use the data collected one cycle prior to treatment.

Lomb–Scargle periodograms. The mathematical framework of this method is described in Section 2. Here we would like to make some remarks about the numerical algorithm and to include all the data sets satisfying the criterion of statistical significance  $p \leq 0.05$ . The corresponding Lomb–Scargle periodograms are also presented (Figs. A1–A7). A crucial ingredient in calculating the false alarm probability is the choice of the number of independent frequencies  $M$ . Horne and Baliunas (1986) performed numerical experiments for determining  $M$  in different situations and concluded that  $M \approx N$  when the data points are approximately equally spaced (as in the platelet counts collected from the CT patients) or the sample frequencies oversample the frequency range. Press et al. (1993) provided an effective way of computing  $M$  under the assumption that there is no important clumping and we used a Matlab implementation of their algorithm.

### Appendix B. Numerical simulations of the CT data

Over time, various therapeutic measures have been tried (the reader is referred to Go (2005) for a comprehensive review). Although no reliable therapy has been established yet, the type of treatment and the drug dose might influence the pattern of platelet oscillations (see Cohen and Cooney, 1974, for the temporal evolution of the platelet levels in a young female subjected to different therapies). For this reason, in the case of the child with chronic thrombocytopenia purpura reported by Aranda and Dorantes (1977) we consider only the data collected under a constant dose of prednisone (it is generally believed that prednisone does not alter the platelet cycles). Given

the variety of the data published in the literature, firstly we focus on the time series corresponding to the patients without any treatment, secondly on the cases when the

therapy does not alter the platelet cycles and, in the end, on the situations when the patient was under diverse treatment (Figs. B1, B2).

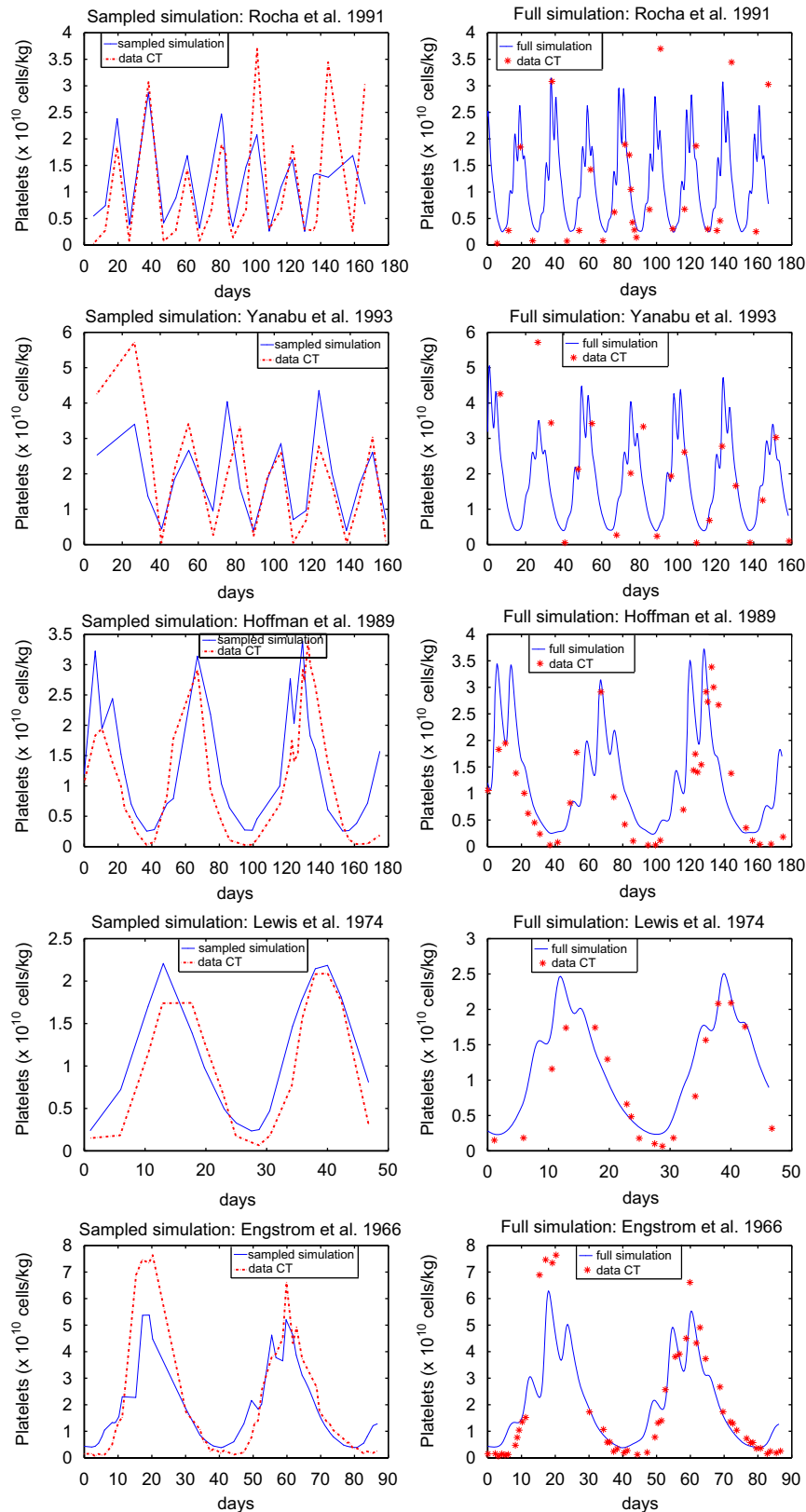


Fig. B1. Output of the simulated annealing fitting and the published platelet data. Sampled (left) and full (right) simulation.

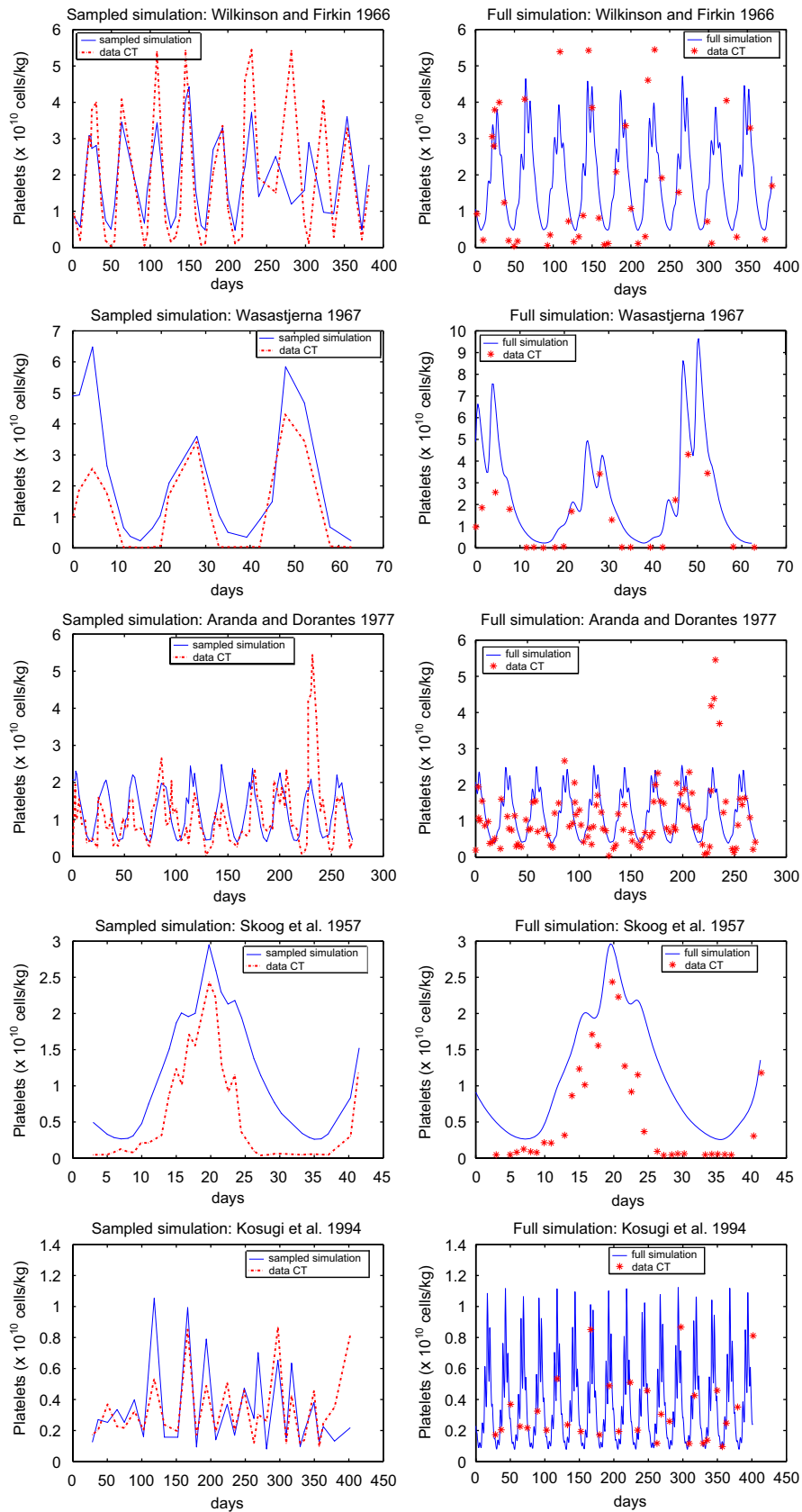


Fig. B2. Output of the simulated annealing fitting and the published platelet data. Sampled (left) and full (right) simulation.

## References

- Apostu, R., 2007. Understanding cyclical thrombocytopenia: a mathematical modeling approach. Master's thesis, Department of Mathematics and Statistics, McGill University.
- Aranda, E., Dorantes, S., 1977. Garcia's disease: cyclic thrombocytopenic purpura in a child and abnormal platelet counts in his family. *Scand. J. Haematol.* 18, 39–46.
- Bélair, J., Mackey, M.C., 1987. A model for the regulation of mammalian platelet. *Ann. N.Y. Acad. Sci.* 504, 280–282.
- Bélair, J., Mackey, M.C., Mahaffy, J.M., 1995. Age-structured and two-delay models for erythropoiesis. *Math. Biosci.* 128, 317–346.
- Bernard, S., Bélair, J., Mackey, M.C., 2003. Oscillations in cyclical neutropenia: New evidence based on mathematical modeling. *J. Theor. Biol.* 223, 283–298.
- Beutler, E., Lichtman, M.A., Coller, B.S., Kipps, T.J., 1995. *Williams Hematology*. McGraw-Hill, New York.
- Branehog, I., Kutti, J., Ridell, B., Swolin, B., Weinfeld, A., 1975. The relation of thrombokinetics to bone marrow megakaryocytes in idiopathic thrombocytopenic purpura (ITP). *Blood* 45, 552–562.
- Bruin, M., Tijssen, M.R., Bierings, M., de Haas, M., 2005. Juvenile cyclic amegakaryocytic thrombocytopenia: a novel entity. *J. Pediatr. Hematol. Oncol.* 27 (3), 148–152.
- Cohen, T., Cooney, D.P., 1974. Cyclic thrombocytopenia. Case report and review of literature. *Scand. J. Haematol.* 12, 9–17.
- Colijn, C., Mackey, M.C., 2005a. A mathematical model of hematopoiesis: Cyclical neutropenia, part II. *J. Theor. Biol.* 237, 133–146.
- Colijn, C., Mackey, M.C., 2005b. A mathematical model of hematopoiesis: Periodic chronic myelogenous leukemia, part I. *J. Theor. Biol.* 237, 117–132.
- Colijn, C., Mackey, M.C., 2007. Bifurcation and bistability in a model of hematopoietic regulation. *SIAM J. Appl. Dynam. Sys.* 6, 378–394.
- Engstrom, K., Lundquist, A., Soderstrom, N., 1966. Periodic thrombocytopenia or tidal platelet dysgenesis in a man. *Scand. J. Haemat.* 3, 290–292.
- Ermentrout, B., 2002. *Simulating, Analyzing, and Animating Dynamical Systems: A Guide to XPPAUT for Researchers and Students (Software, Environments, Tools)*, first ed. SIAM, Philadelphia, PA.
- Fogarty, P.F., Stetler-Stevenson, M., Pereira, A., Dunbar, C.E., 2005. Large granular lymphocytic proliferation-associated cyclic thrombocytopenia. *Am. J. Hematol.* 79, 334–336.
- Foley, C., Bernard, S., Mackey, M.C., 2006. Cost-effective G-CSF therapy strategies for cyclical neutropenia: mathematical modelling based hypotheses. *J. Theor. Biol.* 238, 754–763.
- Fortin, P., Mackey, M.C., 1999. Periodic chronic myelogenous leukaemia: spectral analysis of blood cell counts and aetiological implications. *Brit. J. Haematol.* 104, 336–345.
- Füreder, W., Mitterbauer, G., Thalhammer, R., Geissler, K., Panzer, S., Krebs, M., Simonitsch-Klupp, I., Sperr, W.R., Lechner, K., Kyrle, P.A., 2002. Clonal T cell-mediated cyclic thrombocytopenia. *Brit. J. Haematol.* 119, 1059–1061.
- Furuyama, H., Koga, Y., Hamasaki, K., Kuroki, F., Itami, N., Ishikawa, Y., 1999. Effective treatment of cyclic thrombocytopenia with cepharanthin. *Pediatr. Int.* 41, 584–585.
- Glass, L., Mackey, M.C., 1988. *From Clock to Chaos*. Princeton University Press.
- Go, R.S., 2005. Idiopathic cyclic thrombocytopenia. *Blood Rev.* 19, 53–59.
- Haurie, C., Dale, D.C., Mackey, M.C., 1998. Cyclical neutropenia and other periodic hematological diseases: A review of mechanisms and mathematical models. *Blood* 92, 2629–2640.
- Haurie, C., Dale, D.C., Mackey, M.C., 1999. Occurrence of periodic oscillations in the differential blood counts of congenital, idiopathic and cyclical neutropenic patients before and during treatment with G-CSF. *Exp. Hematol.* 27, 401–409.
- Haurie, C., Dale, D.C., Rudnicki, R., Mackey, M.C., 2000. Modeling complex neutrophil dynamics in the Grey Collie. *J. Theor. Biol.* 204, 505–519.
- Hearn, T., Haurie, C., Mackey, M.C., 1998. Cyclical neutropenia and the peripheral control of white blood cell production. *J. Theor. Biol.* 192, 167–181.
- Helleberg, C., 1995. Cyclical thrombocytopenia successfully treated with low dose hormonal contraception. *Am. J. Hematol.* 48, 62–63.
- Hoffman, R., Briddell, R., van Besien, K., Srour, E., Guscar, T., Hudson, N., Ganser, A., 1989. Acquired cyclical amegakaryocytic thrombocytopenia associated with an immunoglobulin blocking the action of granulocytemacrophage colony-stimulating factor. *N. Engl. J. Med.* 312, 97–102.
- Horne, J.H., Baliunas, S.L., 1986. A prescription for period analysis of unevenly sampled time series. *Astrophys. J.* 302, 757–763.
- Kimura, F., Nakamura, Y., Sato, K., Wakimoto, N., 1996. Cyclic change of cytokines in a patient with cyclical thrombocytopenia. *Brit. J. Haematol.* 94, 171–174.
- Kirkpatrick, S., Gelatt, C.D., Vecchi, M.P., 1983. Optimization by simulated annealing. *Science* 220, 671–680.
- Kosugi, S., Tomiyama, Y., Shiraga, M., Kashiwagi, H., Nakao, H., Kanayama, Y., Kurata, Y., Matsuzawa, Y., 1994. Cyclic thrombocytopenia associated with IgM anti-GPIIb-IIa autoantibodies. *Brit. J. Haematol.* 88, 809–815.
- Lewis, M.L., 1974. Cyclical thrombocytopenia: a thrombopoietin deficiency? *J. Clin. Path.* 27, 242–246.
- Lomb, N.R., 1976. Least-squares frequency analysis of unequally spaced data. *Astrophys. Space Sci.* 39, 447–462.
- Mackey, M.C., 1978. Unified hypothesis for the origin of aplastic anemia and periodic hematopoiesis. *Blood* 51, 941–956.
- Mackey, M.C., 1979. Periodic auto-immune hemolytic anemia: An induced dynamical disease. *Bull. Math. Biol.* 41, 829–834.
- Mackey, M.C., 2001. Cell kinetic status of hematopoietic stem cells. *Cell Prolif.* 34, 71–83.
- Mackey, M.C., Glass, L., 1977. Oscillation and chaos in physiological control systems. *Science* 197, 287–289.
- Mahaffy, J.M., Bélair, J., Mackey, M.C., 1998. Hematopoietic model with moving boundary condition and state dependent delay: Applications in erythropoiesis. *J. Theor. Biol.* 190, 135–146.
- Menitove, J.E., Pereira, J., Hoffman, R., Anderson, T., Fried, W., Aster, R.H., 1989. Cyclical thrombocytopenia of apparent autoimmune etiology. *Blood* 73, 1561–1569.
- Minot, G.S., 1936. Purpura hemorrhagica with lymphocytosis: an acute type and an intermenstrual type. *Am. J. Med. Sci.* 192, 445–456.
- Morley, A., 1969. A platelet cycle in normal individuals. *Aust. Ann. Med.* 18, 127–129.
- Nagasawa, T., Hasegawa, Y., Kamoshita, M., et al., 1998. Serum thrombopoietin level is mainly regulated by megakaryocyte mass rather than platelet mass in human subjects. *Brit. J. Haematol.* 101, 242–244.
- Press, W.H., Flannery, B.P., Vetterling, W.T., Teukolsky, S.A., 1993. *Numerical recipes in C*, second ed. Cambridge University Press, Cambridge.
- Pujo-Menjouet, L., Bernard, S., Mackey, M.C., 2005. Long period oscillations in a g0 model of hematopoietic stem cells. *SIAM J. Appl. Dynam. Sys.* 4 (2), 312–332.
- Rice, L., Nichol, J.L., McMillan, R., Roskos, L.K., Bacile, M., 2001. Cyclic immune thrombocytopenia responsive to thrombopoietic factor therapy. *Am. J. Hematol.* 68, 210–214.
- Rocha, R., Horstman, L., Ahn, Y.S., Mylvaganam, R., Harrington, W.J., 1991. Danazol therapy for cyclic thrombocytopenia. *Am. J. Hematol.* 36, 140–143.
- Salamon, P., Sibani, P., Frost, R., 2002. *Facts, Conjectures, and Improvements for Simulated Annealing*. SIAM, Philadelphia, PA.
- Santillán, M., Bélair, J., Mahaffy, J.M., Mackey, M.C., 2000. Regulation of platelet production: the normal response to perturbation and cyclical platelet disease. *J. Theor. Biol.* 206, 585–603.

- Scargle, J.D., 1982. Studies in astronomical time series analysis, II. Statistical aspects of spectral analysis of unevenly spaced data. *Astrophys. J.* 263, 835–853.
- Skoog, W., Lawrence, J.S., Adams, W.S., 1957. A metabolic study of a patient with idiopathic cyclical thrombocytopenic purpura. *Blood* 12, 844–856.
- Swinburne, J., Mackey, M.C., 2000. Cyclical thrombocytopenia: Characterisation by spectral analysis and a review. *J. Theor. Med.* 2, 81–91.
- Tomer, A., Schreiber, A.D., McMillan, R., Cines, D.B., Burnstein, S.A., Thiessen, A.R., Harker, L.A., 1989. Menstrual cyclic thrombocytopenia. *Brit. J. Haematol.* 71, 519–524.
- Von Schulthess, G.K., Gessner, U., 1986. Oscillating platelet counts in healthy individuals: Experimental investigation and quantitative evaluation of thrombocytopenic feedback control. *Scand. J. Haematol.* 36, 473–479.
- Wasastjerna, C., 1967. Cyclical thrombocytopenia of acute type. *Scand. J. Haematol.* 4, 380–384.
- Wilkinson, T., Firkin, B., 1966. Idiopathic cyclical acute thrombocytopenic purpura. *Med. J. Aust.* 1, 217–219.
- Yanabu, M., Nomura, S., Kukuroi, T., et al., 1993. Periodic production of antiplatelet autoantibody directed against GPIIIa in cyclic thrombocytopenia. *Acta Haematol.* 89, 155–159.
- Zent, C.S., Ratajczak, J., Ratajczak, M.Z., Anastasi, J., Hoffman, P.C., Gewirtz, A.M., 1999. Relationship between megakaryocyte mass and serum thrombopoietin levels as revealed by a case of cyclic amegakaryocytic thrombocytopenic purpura. *Brit. J. Haematol.* 105, 452–458.